Int J Clin Exp Pathol 2020;13(7):1867-1872
www.ijcep.com /ISSN:1936-2625/IJCEP0113956

Original Article

Alveolar macrophages in patients with non-small cell lung cancer

Jinfeng Li[1*], Jinlong Li[2*], Lingxiong Wang[1], Jianqing Hao[3], Liangliang Wu[1], Haitao Tao[1], Sujie Zhang[1], Pengfei Cui[1], Xiaoyan Li[1], Xiaoyun Zhang[1], Zhou Zhou[1], Shunchang Jiao[1], Yi Hu[1]

Departments of [1]Oncology, [2]Pathology, First Department of Medical Oncology, Chinese PLA General Hospital, Beijing, China; [3]Qingyang People's Hospital, Qingyang, Gansu Province, China. [*]Equal contributors.

Received May 7, 2020; Accepted June 11, 2020; Epub July 1, 2020; Published July 15, 2020

Abstract: Objective: To observe alveolar macrophages (AMs) in the microenvironment of patients with non-small cell lung cancer (NSCLC). Materials and Methods: 20 NSCLC patients received bronchoalveolar lavage, and the bronchial alveolar lavage fluid (BALF) was collected. The phenotypes of AMs were detected by the opal multiplex immunofluorescence assay (mIF), flow cytometry, and western blot. Results: AMs could easily be made into paraffin sections after agar pre-embedding. The mIF results showed that AMs highly expressed M1-type marker CD86, and M2-type marker CD163 under PerkinElmer Vectra microscope, while there was a significant difference between the expression of CD86 and CD163 (**P<0.01), consistent with the flow cytometry results. Western blot revealed that the other markers of M1-type (CD16 and iNOS) expression in the AMs were compared with M2-type markers CD206 and ARG (*P<0.05). Conclusions: Our results showed that AMs simultaneously expressed M1-type markers and M2-type markers, while the M2 markers still dominated. This suggests agar pre-embedding is a very convenient method to embed cells to paraffin tissue, so that cell membrane or nuclear antigens are very easily detected by mIF.

Keywords: Non-small cell lung cancer, alveolar macrophages, broncho-lavage alveolar fluid, opal multiplex immunofluorescence assay

Introduction

Lung cancer is the leading cause of cancer-related death worldwide with a high annual incidence and a 5-year survival rate <20% [1, 2]. Non-small cell lung cancer (NSCLC) accounts for approximately 85% of lung cancer and represents a heterogeneous group of cancers, consisting mainly of adeno (AC), squamous cell (SCC), and large-cell carcinoma [1, 2]. The fiber-optic bronchoscopy has provided a more intuitive and scientific basis for the early diagnosis of lung cancer [3]. Besides biopsy specimens, cytology samples can be obtained through bronchoscopes, sterile saline can be rinsed repeatedly the alveoli of the lung cancer patients to obtain the broncho-lavage alveolar fluid (BALF) [4]. Alveolar macrophages (AMs) account for about 90% of BALF, and play an important role in the development and metastasis of lung cancer [5-7]. As macrophages, AMs also are divided into M1-type (classical activated macrophages) and M2-type (alternative activated macrophages), and also express the PD-L1 (CD274) [6-8]. The observation of AMs is beneficial to the analysis of alveolar microenvironment of NSCLC patients [9]. In Domagala-Kulawik's overview, BALF analysis may replace cancer tissue examination, for the recognition of the nature of immune response in the tumor environment, especially at advanced stages [10].

In this study, we used several different methods to analyze the phenotypes of AMs in BALF. Flow cytometry is the gold standard for phenotyping and quantifying the immune cells. We attempted to make AMs to paraffin-embedded specimens using agar pre-embedding by referring to Ridolfi's report [11], and then detected the phenotypes of AMs by the opal multiplex immunofluorescence assay (mIF), a new and ingenious method for immune-profiling in cancer patients. The mIF perfectly showed that AMs simultaneously highly expressed the M1-type markers and M2-type markers in situ,

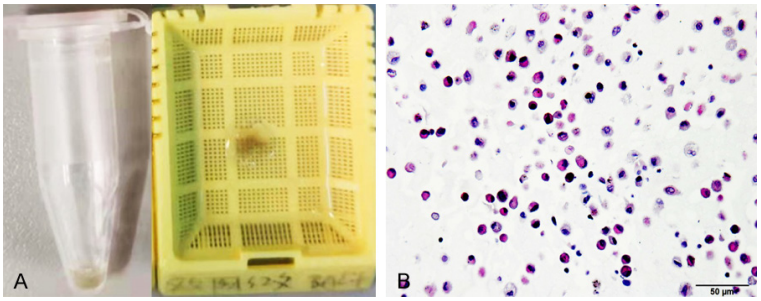

Figure 1. A: The cells and agar mixture in an EP tube and the tissue cassette. B: The H&E staining of agar pre-embedding paraffin section showed the complete cell morphology of AMs (bar = 50 μm).

consistent with the results of flow cytometry and western blot. Therefore, our results revealed that M2-like AMs with immunosuppressive properties are abundant in the alveolar microenvironment, although these AMs also highly expressed the M1-type markers.

Materials and methods

Patients

A group of 20 patients with confirmed primary NSCLC was investigated (14 AC, 6 SCC). 20 BALF samples were collected from patients in the bronchoscopy section from June 2018 to October 2019 in the General Hospital of PLA. Their mean age was 67.8 years (range 47-79 years). Written informed consent was taken from all participants. Collection of samples was all approved by the Ethics Committee of Chinese PLA General Hospital. Lung cancer was diagnosed by either histologic examination of tissue specimens or cytologic examination of sputum, or specimens obtained by bronchial brushing, lymph node biopsy, or lung aspiration.

Collection of BALF

Fiberoptic bronchoscopy (Olympus BF20D) with BALF was performed in accordance with the British Thoracic Society Guidelines for advanced diagnostic and therapeutic flexible bronchoscopy in adults [4]. The sampling area was selected based on the infiltrate location on the chest radiograph. Then, 80 ml sterile normal saline was injected through the device four times. The suction channel of the bronchoscope was used to aspirate 25-30 ml fluid, yielding clinical samples, which were collected into sterile tubes and immediately transferred to the laboratory. All BALF samples were centrifuged for 10 minutes (min) at 1000 revolutions per minute (r.p.m.). The supernatants were removed and stored at -80°C. We added 1000 μl sterile distilled water to centrifuge the tube and blended again, and absorbed 500 μl for flow cytometry. After re-centrifugation, the remaining sediment was fixed with 4% neutral buffered formalin (about 0.5-1 × 10^6 cells).

Agar pre-embedding

The agar (0.2 g) and 10 ml distilled water was mixed in a glass plate and heated until melted. After solidification, the agar was divided into tiny pieces and stored at 4°C. The cells were washed with PBS one time after discarding the neutral formalin. After centrifugation, the remaining sediment and a small piece of agar was re-heated until melted. The cells and agar mixture were picked from the EP tube when these cooled, and then transferred to the tissue cassette (**Figure 1A**). After routine processing, the agar pre-embedded tissue was finally embedded in paraffin and subsequently slides were made by microtome for H&E staining (**Figure 1B**) and mIF.

mIF

The panel of AMs markers were CD45 (Abcam, Cambridge UK, ab214437, 1:800), CD68 (Genomic Technology co. LTD, Shanghai, China, 1:800), CD86 (Abcam, Cambridge UK, ab209896, 1:800), CD163 (Genomic Technology co. LTD, China, Shanghai, 1:800), and PD-L1 (Genomic Technology co. LTD, Shanghai, China, 1:1000). The tissue was de-paraffinized and underwent heat-mediated antigen retrieval in citrate buffer prior to triple labeling with the Opal Multiplex Immunostaining kit (Perkin Elmer, Waltham, MA). Briefly, slides were rinsed with TBST for 10 min, incubated in 1% bovine serum albumin for 30 min at room temperature (RT), and incubated with the anti-CD45 primary antibody for 2 h followed by washing with TBST (3 × 2 min). Slides were incubated with secondary antibody (Genomic technology co. LTD, Shanghai, China) for 30 min at RT, washed with TBST (3 × 2 min), incubated with the Opal 520 fluorophore working solution (1:300) for 10 min at RT, and

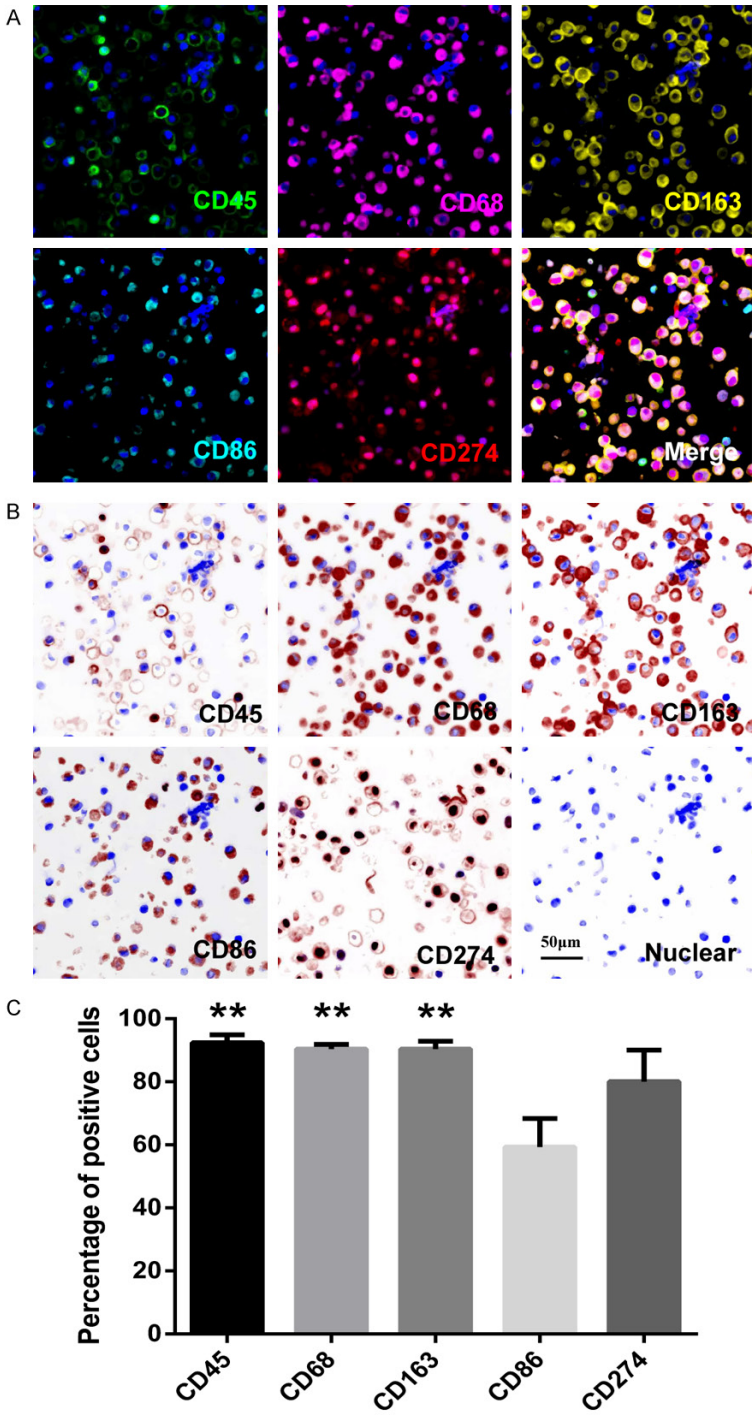

Figure 2. A: Results of mIF for agar pre-embedding paraffin section of AMs showed CD45 (green), CD68 (rose), CD163 (yellow), CD86 (cyan), CD274 (red), and nuclei stained with DAPI (blue). B: The expression of CD45, CD68, CD86, CD163, CD274 and nuclear in bright-field (all pictures bar = 50 μm). C: Statistical analysis showed there was a significant difference between the expression of CD86 and CD45, CD68, and CD163 (***P*<0.01, two-way analysis of variance, Bonferroni's multiple comparisons test).

washed with TBST (3 × 2 min). Slides then underwent heat-mediated antigen retrieval and antibody removal in citrate buffer. After cooling, the process was repeated for two additional rounds for labeling with anti-CD68, CD86, CD163, and PD-L1 followed by secondary labeling with the respective fluorophore working solution [ie, Opal 570 (1:300), Opal 650 (1:500), Opal 690 (1:300) and Opal 620 (1:1000), respectively, (PerkinElmer, Waltham, MA)] as described above. Next, nuclei were labeled with DAPI for 10 min in a humid chamber, washed with dH_2O, and coverslips were mounted with glycerin. Upon completion of multiplex IF staining, the slides were imaged using the Vectra 3.0 spectral imaging system (Perkin-Elmer). The chromogenic IHC-stained slides were scanned by using the bright field protocol, and the uniplex and multiplex IF staining was imaged by using the fluorescence protocol at 10 nm λ from 420 nm to 720 nm, to extract fluorescent intensity information from the images. A similar approach was used to build the spectral library using the InForm 2.2.1 image analysis software (PerkinElmer).

Flow cytometry

AMs were incubated with CD45-APC-Cy7, CD86-PE, CD163-Pacific Blue, and CD274-PE-Cy7 antibodies in the dark at 4°C for 30 min (all antibodies from BD Pharmingen™, United States). Intracellular CD68 staining of AMs was subsequently performed according to the manufacturer's instructions after fixation and permeabilization (eBioscience, United States). Images of stained cells were acquired using a Gallios flow cytometer (Beckman Coulter, United States) and analyzed with Flowjo v.7.6.1 software.

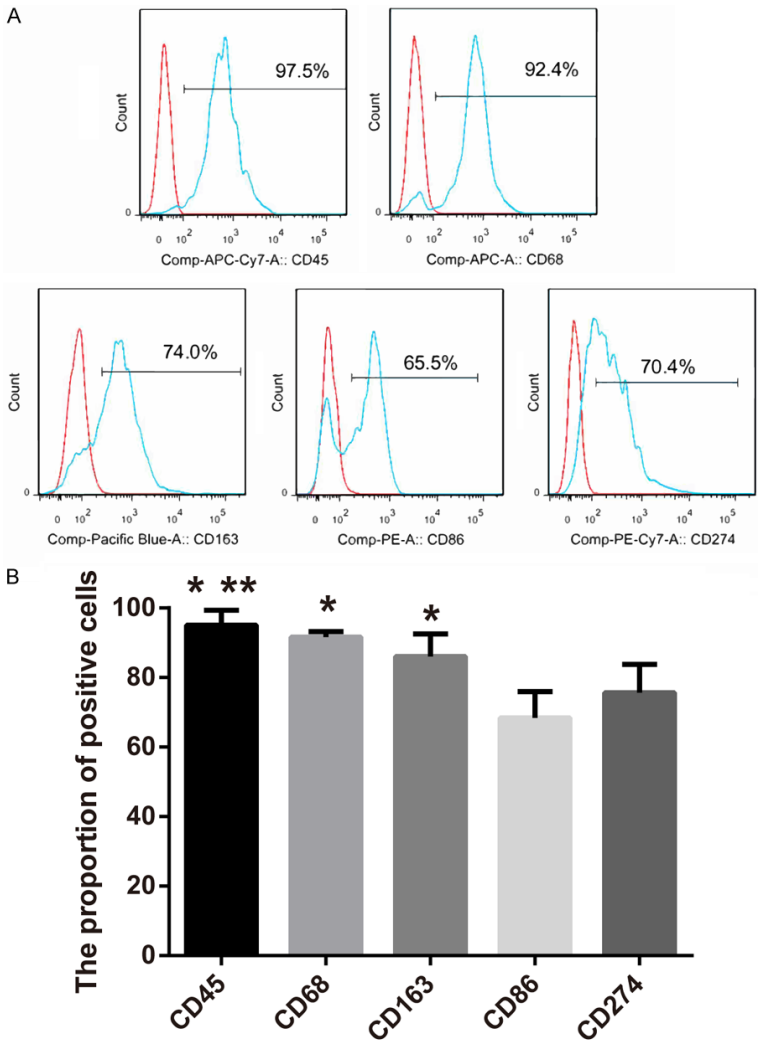

Figure 3. A: Cell markers of AMs were assessed using flow cytometer. Almost all cells in BALF expressed CD45; the percentages of CD68+, CD163+, CD86+, and CD274+ cells in BALF were respectively about 90%, 75%, 65%, and 70%. B: There was a significant difference between the expression of CD86 and CD45, CD68, and CD163 (*P<0.05, **P<0.01, two-way analysis of variance, Bonferroni's multiple comparisons test). The expression of CD45 was also different from that of CD274 (b, *P<0.05, one-way analysis of variance).

Western blot

AMs are lysed mechanically with sonication, and then a low-speed centrifugation (700 g) was used to remove large cellular debris. Supernatant from this step is collected as a total lysed protein fraction. The proteins were separated by SDS-PAGE electrophoresis and transferred to polyvinylidene difluoride (PVDF) membranes (R&D System, Minneapolis, MN, USA). The membranes were blocked with 5% nonfat dry milk in Tris buffered saline (TBS) with Tween (TBST; TBS plus 0.1% Tween 20) for 1 h and incubated with primary antibodies overnight at 4°C. The following primary antibodies were used: CD45, CD68, CD206, ARG, CD16, and iNOS (rabbit IgG, 1:1000, Abcam, Cambridgeshire, UK). The following secondary antibodies were used: goat anti-rabbit IgG/HRP (1:5,000, Golden Bridge International, Beijing, China); and rabbit anti-goat IgG/HRP (1:5,000, Golden Bridge International, Beijing, China). The intensity of the bands was quantified using the Image J software. The level of expression for the target protein was calculated as the ratio of the band intensity of the target protein over that of β-actin.

Statistical analysis

Statistical analyses were performed using SPSS 10.0 (SPSS Inc., USA). Data are presented as means ± SEM and tested using two-way analysis of variance followed by either the Newman-Keuls or Bonferroni's multiple-comparisons test as a post hoc test. P<0.05 was considered significant. In this study, all experiments were performed three times and the mean values were used for analysis. The positive cell fluorescence staining of mIF was analyzed by inForm 2.2.1 image analysis software (PerkinElmer). The results of western blot were analyzed by Image-ProPlus 5.0 image analyzer (Media Cybernetics, USA). The relative abundance was evaluated by statistical analysis.

Results

Analysis of AMs markers by mIF

In agar pre-embedding paraffin section, about 90% cells of BALF expressed leukocyte common antigen CD45 (green fluorescence). The specific marker of macrophages CD68 (rose

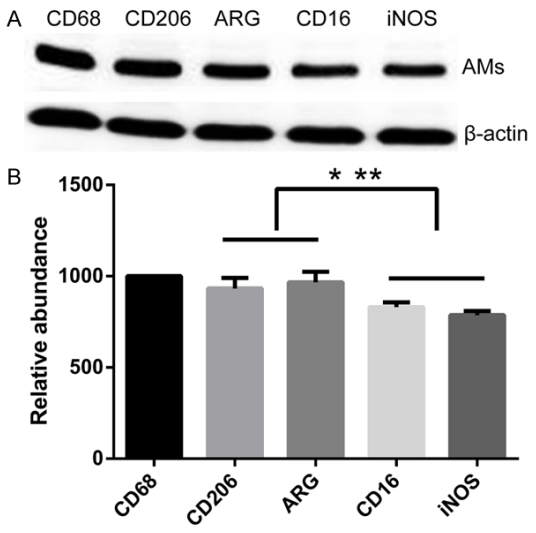

Figure 4. A: AM markers were analyzed by western blot. B: There was a significant difference between the expression of the specific markers of M1-type (CD16 and iNOS) and M2-type (CD206 and ARG) AMs (*P<0.05: CD16 vs. CD206 and ARG, **P<0.01: iNOS vs. CD206 and ARG, two-way analysis of variance, Bonferroni's multiple comparisons test).

fluorescence) mainly existed in the cytoplasm of $CD45^+$ cells. Almost all $CD68^+$ cells expressed the M2-type surface marker CD163 (yellow fluorescence), and some cells simultaneously expressed M1-type surface marker CD86 (cyan fluorescence). The results of mIF seemed to suggest that CD274 (red fluorescence) was expressed not only in the cell membrane, but also in the nucleus of AMs (**Figure 2A**). The bright-field results also clearly corresponded to mIF (**Figure 2B**). The positive cell fluorescence staining was analyzed by inForm 2.2.1 image analysis software. There was a significant difference between the expression of CD86 and of CD45, CD68, CD163 (**Figure 2C**, **P<0.01).

Analysis of AMs markers by flow cytometry

Common cell markers of AMs were carried out using flow cytometer. The percentages of $CD45^+$ cells in BALF are about 98%. CD45, leukocyte common antigen, is expressed on almost all hematopoietic cells except for mature erythrocytes, besides AMs. The epithelial cells do not express CD45. AMs dominate in BALF, so the percentages of CD68+ cells in AMs were about 90%. The percentages of CD163, CD86, and CD274 were respectively about 75%, 65%, and 70% (**Figure 3A**). There was a significant difference between the expression of CD86 and of CD45, CD68, and CD163 (**Figure 3B**, *P<0.05, **P<0.01). The expression of CD45 was also different from that of CD274 (*P<0.05).

Western blot

The other specific markers of M1-type (CD16 and iNOS) and M2-type (CD206 and ARG) AMs were detected by western blot (**Figure 4A**). Results of western blot showed that CD16 and iNOS expression in the AMs were decreased compared with CD206 and ARG (**Figure 4B**, *P<0.05: CD16 vs. CD206 and ARG, **P<0.01: iNOS vs. CD206 and ARG).

Discussion

In recent years, immunotherapy has become an innovative technology for NSCLC therapy with the discovery of immunological checkpoints (ICIs). However, ICIs are associated with a constellation of toxicities termed immune-related adverse events (irAEs); the most common is checkpoint inhibitor pneumonitis (CIP) [12-14]. Lymphocytes were often specifically detected and observed in CIP [15]. AMs are the most abundant innate immune cells in the distal lung parenchyma, located on the luminal surface of the alveolar space, which indicates that AMs play a central role in the development of lung cancer and CIP [16, 17]. It has been reported that E3 ligase von Hippel-Lindau protein (VHL) acts as a crucial regulatory factor in lung inflammation and fibrosis by regulating AMs [18]. In order to explore the mechanism of CIP, our team will focus on AMs in BALF of NSCLC patients.

We firstly used several methods to detect the phenotype of AMs to prepare for the next experiment in this study. Our results showed that AMs simultaneously expressed the M1-type markers CD86, CD16, iNOS, and the M2-type markers CD163, CD206, and ARG. Although there were some differences between M1-type marker expression and M2-type marker expression, no specific markers had been found to exactly distinguish M1-type AMs from M2-type AMs.

We attempted to make AMs into agar-paraffin sections to facilitate to analyze the changes in cell phenotypes and some transcription factors in cells in this study. Our results showed that AMs in agar-paraffin sections could be easily marked by common marker antibodies by mIF and immunohistochemical staining because of antigen retrieval. The percentage of positive

cells was generally consistent with the data from flow cytometry. About 1×10^5 cells, maybe even fewer, also can be made into agar paraffin sections successfully. The agar paraffin can be cut a dozen or even dozens of sections. The cell specimens in paraffin are easier to preserve. Therefore, our study provides an innovative method for observation and long-term preservation of cell samples. We will continue to use this method in future experiments.

Acknowledgements

This work was supported by the National Natural Science Foundation of China, Grant/Award Number: 81402552 and 81672996.

Disclosure of conflict of interest

None.

Address correspondence to: Yi Hu and Shunchang Jiao, Department of Oncology, First Department of Medical Oncology, Chinese PLA General Hospital, Beijing, China. E-mail: huyi0401@aliyun.com (YH); jiaosc@vip.sina.com (SCJ)

References

[1] Siegel RL, Miller KD and Jemal A. Cancer statistics, 2019. CA Cancer J Clin 2019; 69: 7-34.

[2] Chen JL, Han HN, Lv XD, Ma H, Wu JN and Chen JR. Clinical value of exhaled breath condensate let-7 in non-small cell lung cancer. Int J Clin Exp Pathol 2020; 13: 163-171.

[3] Yasukawa M, Sawabata N, Kawaguchi T, Kawai N and Taniguchi S. Clinical implications of transbronchial biopsy for surgically-resected non-small cell lung cancer. In Vivo 2018; 32: 691-698.

[4] Du Rand IA, Barber PV, Goldring J, Lewis RA, Mandal S, Munavvar M, Rintoul RC, Shah PL, Singh S, Slade MG and Woolley A; BTS Interventional Bronchoscopy Guideline Group. Summary of the british thoracic society guidelines for advanced diagnostic and therapeutic flexible bronchoscopy in adults. Thorax 2011; 66: 1014-1015.

[5] Brcic L, Stanzer S, Krenbek D, Gruber-Moesenbacher U, Absenger G, Quehenberger F, Valipour A, Lindenmann J, Stoeger H, Al Effah M, Fediuk M, Balic M and Popper HH. Immune cell landscape in therapy-naive squamous cell and adenocarcinomas of the lung. Virchows Arch 2018; 472: 589-598.

[6] Joshi N, Walter JM and Misharin AV. Alveolar macrophages. Cell Immunol 2018; 330: 86-90.

[7] Milette S, Fiset PO, Walsh LA, Spicer JD and Quail DF. The innate immune architecture of lung tumors and its implication in disease progression. J Pathol 2019; 247: 589-605.

[8] Mukaida N, Nosaka T, Nakamoto Y and Baba T. Lung macrophages: multifunctional regulator cells for metastatic cells. Int J Mol Sci 2018; 20: 1-15.

[9] Lommatzsch M, Bratke K and Stoll P. Neoadjuvant PD-1 blockade in resectable lung cancer. N Engl J Med 2018; 379: e14.

[10] Domagala-Kulawik J. New frontiers for molecular pathology. Front Med (Lausanne) 2019; 6: 284.

[11] Ridolfi M, Paudice M, Salvi S, Valle L, Gualco M, Perasole A, Anselmi L, Fiocca R, Mastracci L and Grillo F. Agar pre-embedding of small skin biopsies: real-life benefits and challenges in high throughput pathology laboratories. J Clin Pathol 2019; 72: 448-451.

[12] Cui P, Liu Z, Wang G, Ma J, Qian Y, Zhang F, Han C, Long Y, Li Y, Zheng X, Sun D, Zhang J, Cai S, Jiao S and Hu Y. Risk factors for pneumonitis in patients treated with anti-programmed death-1 therapy: a case-control study. Cancer Med 2018; 7: 4115-4120.

[13] Chuzi S, Tavora F, Cruz M, Costa R, Chae YK, Carneiro BA and Giles FJ. Clinical features, diagnostic challenges, and management strategies in checkpoint inhibitor-related pneumonitis. Cancer Manag Res 2017; 9: 207-213.

[14] Larsen BT, Chae JM, Dixit AS, Hartman TE, Peikert T and Roden AC. Clinical and histopathologic features of immune checkpoint inhibitor-related pneumonitis. Am J Surg Pathol 2019; 43: 1331-1340.

[15] Tanaka K, Yanagihara T, Ikematsu Y, Inoue H, Ota K, Kashiwagi E, Suzuki K, Hamada N, Takeuchi A, Tatsugami K, Eto M, Ijichi K, Oda Y, Otsubo K, Yoneshima Y, Iwama E, Nakanishi Y and Okamoto I. Detection of identical T cell clones in peritumoral pleural effusion and pneumonitis lesions in a cancer patient during immune-checkpoint blockade. Oncotarget 2018; 9: 30587-30593.

[16] Sternschein R, Moll M, Ng J and D'Ambrosio C. Immune checkpoint inhibitor-related pneumonitis: incidence, risk factors, and clinical and radiographic features. Am J Respir Crit Care Med 2018; 198: 951-953.

[17] Sears CR, Peikert T, Possick JD, Naidoo J, Nishino M, Patel SP, Camus P, Gaga M, Garon EB, Gould MK, Limper AH, Montgrain PR, Travis WD and Rivera MP. Knowledge gaps and research priorities in immune checkpoint inhibitor-related pneumonitis: an official american thoracic society research statement. Am J Respir Crit Care Med 2019; 200: e31-e43.

[18] Zhang W, Li Q, Li D, Li J, Aki D and Liu YC. The E3 ligase VHL controls alveolar macrophage function via metabolic-epigenetic regulation. J Exp Med 2018; 215: 3180-3193.